

FORMATION OF NANOCARBON SPHERES BY THERMAL TREATMENT OF WOODY CHAR FROM FAST PYROLYSIS PROCESS

Qiangui Yan

Postdoctoral Research Associate
Department of Agricultural & Biological Engineering
Mississippi State University
Mississippi State, MS 39762
E-mail: qy8@ra.msstate.edu

Hossein Toghiani

Associate Professor
Dave C. Swalm School of Chemical Engineering
Mississippi State University
Mississippi State, MS 39762
E-mail: hossein@che.msstate.edu

Zhiyong Cai[†]

Project Leader
USDA Forest Service
Forest Products Laboratory
Madison, WI 53726-2398
E-mail: zcai@fs.fed.us

Jilei Zhang^{*†}

Professor
Department of Forest Products
Mississippi State University
Mississippi State, MS 39762-9820
E-mail: jzhang@cfr.msstate.edu

(Received November 2013)

Abstract. Influences of thermal treatment conditions of temperature, reaction cycle and time, and purge gas type on nanocarbon formation over bio-chars from fast pyrolysis and effects of thermal reaction cycle and purge gas type on bio-char surface functional groups were investigated by temperature-programmed desorption (TPD) and temperature-programmed reduction methods. Nanospheres occurred on bio-chars under the activation temperature of 700°C; more nanospheres occurred when temperature increased to 900°C. Further increase of temperature to 1100°C yielded bio-char surfaces covered with a layer of nanospheres between 20 and 50 nm. More carbon nanospheres formed by increasing thermal cycles and reaction time. Scanning electron microscope images of char surfaces showed there were fewer or no nanoparticles produced using H₂ as the purge gas and they were porous. TPD results indicated that H₂, H₂O, CH₄, CO, and CO₂ in gas phases evolved from chars heated to 1000°C during the first heating cycle. H₂ and CH₄ peaked at 750 and 615°C, respectively. Both H₂O and CO had two peaks, and CO₂ had a broad peak. Only trace amounts of H₂ and CO were detected in the second cycle. There was no detection for CH₄, H₂O, and CO₂ after the second cycle.

Keywords: Pine char, thermal, nanocarbon structures.

* Corresponding author

† SWST member

INTRODUCTION

In addition to diamond and graphite, synthetic carbon materials have been extensively studied for a wide variety of applications for the past decade (Mezohegyi et al 2012). These carbon materials are defined not only by their primary particle sizes on a nanometer scale, but also by their structures and/or textures controlled on the nanometer scale (Qureshi et al 2009). Both nano-sized and nano-structured carbon materials must be prepared under deliberately controlled conditions to yield specific properties and functions (Dasgupta et al 2011). Generally, the nano-sized/nano-structured carbon materials include nanocarbon black, carbon nanotubes (CNT) (Llobet 2013), carbon nanofibers (CNF) (Lubineau and Rahaman 2012), carbon nanocones (Balaban et al 1994), carbon nanospheres (Miao et al 2004), and graphenes (Geim and Novoselov 2007).

Carbon-based nanomaterials can be produced from carbon-containing compounds using thermal, chemical, or hydrothermal processes in their gas, liquid, or solid phases (Hwang 2010). The physical and chemical properties as well as the structure of the formed carbons are affected by the reaction conditions and the feedstock (Pierson 2006). Carbon materials have been widely produced by thermochemical processes in the gas phase. Chemical vapor deposition (CVD) and pyrolysis techniques are the most frequently used methods to form CNF, CNT, carbon films, and carbon blacks. The feedstock of the carbon precursors are selected from carbon-containing gases, eg CO, CH₄, C₂H₂, C₃H₆, C₆H₆, or the vapor phase of biomass pyrolysis. The CVD process usually is promoted by a metallic catalyst such as iron, cobalt, or nickel (Li et al 2004). The thermochemical process is conducted under high temperature (700-1000°C) and low pressure, usually atmospheric pressure. Carbon products can be obtained in liquid-phase reactions using thermoplastic polymers or liquid hydrocarbons under traditional carbonization conditions, typically greater than 2000°C in a largely nonreactive medium. Graphitizable carbon fibers, cokes, and graphite can be produced by this car-

bonization process (Morgan 2005). Carbon materials, eg carbon nanospheres, have been fabricated in the aqueous phase by a hydrothermal process in recent years. The feedstock varies from glucose and alcohols to organic acid molecules (Wang et al 2001). Carbon formation processes can also take place in the solid phase via the thermal decomposition of coals, wood, some polymers, and biomass in nonreactive mediums. Activated carbon, activated carbon fibers, and carbon molecular sieves have been produced by this process (Serp and Figueiredo 2008). However, the raw sources used currently are not sustainable or renewable and the processes are expensive.

Biomass is an abundant and low-cost carbon source for value-added carbonaceous nanoparticle production. However, limited studies have been reported on the use of wood or annual agricultural biomass as the carbon source. In biofuel research, most attention has been concentrated on bio-oil upgrading and syngas formation and use and less attention has been paid to the use of its byproduct wood char, which accounted for 30-50% of the carbon in the wood (Mohan et al 2006). The synthesis of value-added carbonaceous nanomaterials from biochars, and also carbon-rich and renewable biomass such as wood and agriculture plants, can be an attractive option to use carbon resources in a sustainable and "CO₂-neutral" way compared with fossil resources (Hüttinger and Michenfelder 1987). More than 90 wt% of the content in bio-char is elemental carbon. Using bio-chars to fabricate nanocarbon materials will add value to this byproduct and eventually help improve the wood pyrolysis process economics (Yan et al 2013).

Özçimen and Ersoy-Meriçboyu (2008) examined the effect of temperature, sweep gas flow rate, and heating rate on the yield of bio-chars from grape seeds and chestnut shells. It was found that yield decreased with increasing temperature, heating rate, and sweep gas flow rate, and temperature had a significant effect on the bio-char yield compared with nitrogen gas flow rate and heating rate. Dalai and Azargohar

(2007) converted bio-char to activated carbon through physical (steam) and chemical (potassium hydroxide) activation. Azargohar and Dalai (2006) attempted to produce activated carbon from bio-char through chemical activation using potassium hydroxide. Demirbas et al (2006) studied adsorptive properties of activated carbons and fly ashes from Turkish coal and biomass resources. Satya Sai and Ahmed (1997) prepared activated carbons from coconut shell char using steam or CO₂ as the reacting gas in a 100-mm-diameter fluidized bed reactor.

The objectives of this study were to characterize the bio-char from fast pyrolysis of pinewood, understand the structure and surface properties of the bio-char, and investigate the effect of thermal treatment conditions such as temperature, reaction cycle and time, and purge gas type on the nanocarbon formation over the bio-char. The ultimate goal was to find a value-added use for the bio-char, which is a byproduct of the biomass fast pyrolysis process.

MATERIALS AND METHODS

Pretreatment of Char

Bio-char used in this study was obtained from an auger-type fast pyrolysis reactor with a feed stock of southern yellow pine wood chips (Mohan et al 2006). The fast pyrolysis experiments of pine wood chips were performed in a stainless steel auger reactor located at the Department of Forest Products, Mississippi State University. A detailed description of the reactor was reported elsewhere (Ingram et al 2008). The pine wood chips were fed into a cylindrical reactor (76 mm in diameter and 1.02 m long) at the rate of 1 kg/h. The auger rate applied was 12 rpm at a pyrolysis temperature of 450°C. Pyrolysis breaks wood chips into three fractions: vapor, gas, and char. The char was first boiled in 0.1 M HNO₃ solution for 12 h remove any soluble alkali ions, alkaline earth ions, and bio-oil residue. Char was then washed several times using hot deionized H₂O followed by drying in an oven at 105°C for 12 h.

Thermal Treatment of Char

Experiment I was to heat-treat 15 g pretreated char using the setup shown in Fig 1 at three temperatures (700, 900, and 1000°C) with a nitrogen flow under atmospheric pressure to study temperature effects on nanocarbon formation. A Lindberg/Blue tube furnace (Thermo Scientific, White Deer, PA) was used in this work. For each temperature run, the gas flow rate, heating rate, and heating time at the final temperature were 50 mL/min, 10°C/min, and 60 min, respectively. In addition, the pretreated char was heated to 1000°C for extended times of 3 and 5 h.

Experiment II was to heat-treat 200 mg pretreated char to 1000°C using the setup shown in Fig 2 without extended time for one, three, and five cycles. A Lindberg/Blue M Mini-Mite tube furnace (Thermo Scientific) was used in this experiment. All experiments were under a nitrogen atmosphere at a heating rate of 10°C/min with a nitrogen flow rate of 50 mL/min. This experiment was designed to investigate the evolution of surface functional groups such as H₂ ($m/z = 2$), CH₄ ($m/z = 15$ or 16), H₂O ($m/z = 18$), CO or nitrogen ($m/z = 28$), and CO₂ ($m/z = 44$) on the pretreated char and nanocarbons using a temperature-programmed decomposition (TPD) process. The TPD experiment involved heating a sample in a purging gas environment at a programmed heating rate to induce thermal desorption of adsorbed species from the surface.

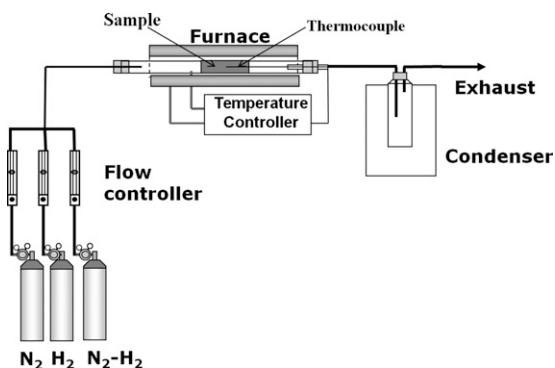


Figure 1. Experiment I setup.

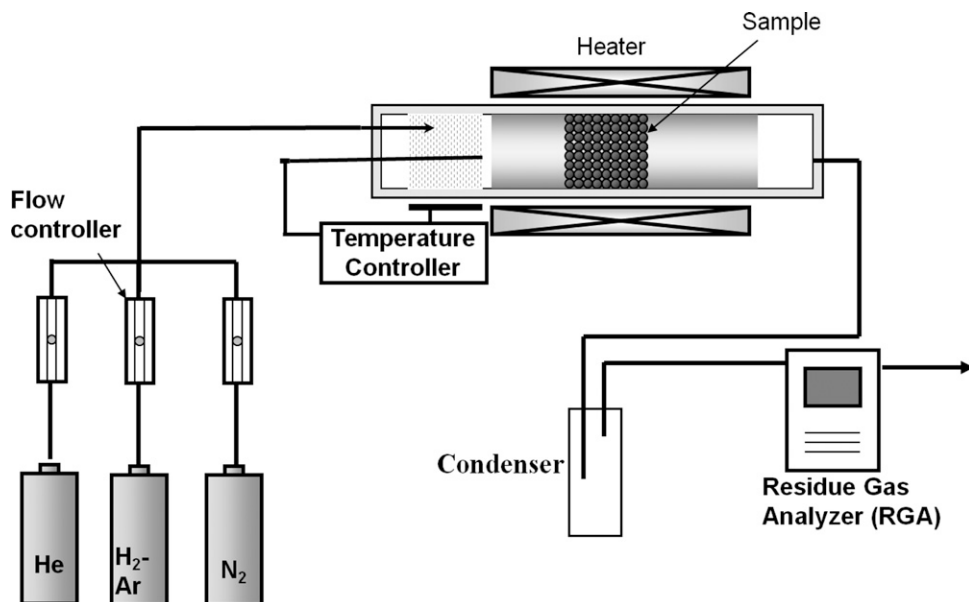


Figure 2. Experiment II and III setup.

The TPD profiles (showing the number of peaks of each species and the temperature of desorption) provide information on the types of species desorbed from the carbon surface, from the decomposition of surface functionalities, and on the nature of interactions of the gaseous species and carbon.

Experiment III was a temperature-programmed reduction (TPR) run performed using the setup shown in Fig 2. The experiment was designed to study the purge gas effect on the surface functional groups present on the char and nanocarbon formation. Each sample of 200 mg pretreated char was first pretreated in helium at 110°C for 1 h and then cooled to room temperature under a helium flow. Then, the helium flow was replaced by a N₂ or 10% H₂ and 90% argon mixture flow at a rate of 50 mL/min as a purging gas. After the concentration of effluent became steady, the temperature was ramped at a rate of 10°C/min to 1000°C without extended hours.

Experiment IV was a thermogravimetric analysis (TGA) performed using TGA 50H to evaluate the weight loss occurring at different temperatures

during the heating process up to 1000°C with a heating rate of 10°C/min and under N₂ atmosphere. For the run, 20 mg of pine char were used.

Characterization of Char and Nanocarbon Samples

Sample morphology was investigated with a scanning electron microscope (SEM) equipped with energy-dispersive X-ray spectroscopy (EDX) (JSM-6500F; JEOL, Peabody, MA). The instrument was coupled to X-EDS and WDS (wavelength dispersive X-ray spectroscopy) spectrometers and Oxford Instruments (Oxfordshire, UK) INCA Energy+ software for electron-beam-induced X-ray elemental analysis. All samples were precoated with 5 nm platinum before being introduced into the vacuum chamber. The system was operated with accelerating voltage of 5-10 kV. Char morphology and particle sizes were also examined with a JEOL JEM-100CX II transmission electron microscopy (TEM) operated at an accelerating voltage of 100 kV. All samples were sonicated in ethanol solution for 20 min before being transferred to copper supports.

RESULTS AND DISCUSSION

Morphology

Effect of temperature. Figure 3 shows the temperature effect on the char morphology. The bio-char (Fig 3b) from fast pyrolysis at 500°C was more porous than the raw pinewood chips (Fig 3a). Nanospheres appeared on the char surface (Fig 3c) at 700°C because of the secondary pyrolysis reactions that continue to break down C-O, C-H, and other C-O bonds to promote carbonization or graphitization of the char. More nanospheres (Fig 3d) occurred when the temperature was raised to 900°C. A further increase of the activation temperature to 1000°C resulted in the carbon material being covered with a layer of nanospheres (Fig 3e). These nanospheres were between 20 and 100 nm.

Figure 4 shows SEM images of bio-char thermally treated at 1000°C with different magnifications. Figure 4a taken at 800× magnification only demonstrated the morphology and microstructure of the char surface. When magnification increased to 5500×, the surface of thermally treated chars was observed to be covered with a layer of nanoparticles (Fig 4b). At 30,000× magnification, these nanoparticles measured between 20 and 100 nm (Fig 4c).

Effect of reaction time. Figure 5 shows SEM images of bio-char thermally treated at 1000°C for 3 extended hours. With the extension of reaction time, carbonization and activation occurred during the thermal activation of the char. The elements (oxygen, nitrogen, and hydrogen) were removed in gaseous form by pyrolytic decomposition of the char. Secondary pyrolytic reactions of char were slow under the conditions studied (1000°C). The C-H bond in aromatic or aliphatic structures was very stable and broke slowly at 1000°C. Oxygen atoms existing as quinone and phenol groups were also firmly combined in the char matrix and decomposed gradually to gaseous CO at 1000°C (Figueiredo et al 1999). With the heating time extended, the freed carbon atoms then recombined and condensed to nano-structured

graphite. Thus, the number of nanocarbon spheres increased with reaction time because of char matrix structure development.

Effect of thermal cycles. Figure 6 shows SEM images of bio-chars thermally treated at 1000°C for different cycles. Images of chars demonstrate more carbon nanospheres formed with increasing thermal cycles. These carbon nanoparticles ranged from 10 to 20 nm. Increasing thermal cycles can improve the productivity of nanocarbon, but it is not as significant as reaction time because this experiment did not hold with the extended time at 1000°C.

Effect of purge gas. Figure 7 shows the SEM image of bio-chars thermally treated at 1000°C with the purging gas of 10% H₂ and 90% argon mixture. There are few or no nanoparticles observed on the char surface because the reaction between carbon and hydrogen occurred at high temperatures (Shahin 1965). Under these conditions, reactions of char with H₂ prevent it from carbonization and secondary pyrolytic reactions. Therefore, H₂ purge gas is detrimental to development of these nanocarbon spheres.

Surface Functional Groups

Effect of thermal cycles. TPD experiments followed by an online residue gas analyzer were conducted to detect gases produced during the thermal activation of pine char. The surface functionalities chemically bound to the char decomposed after heating by releasing gaseous compounds at different temperatures. Interpretation of the thermal desorption profiles provides useful information on the types of species desorbed from the char surface and on the nature of interactions of the gaseous species and carbon. The amounts of these different surface groups can be estimated from the TPD spectra.

Figure 8 shows a typical profile recording the evolution of five species in gas phase: H₂, H₂O, CH₄, CO, and CO₂ when the pine char was heated to 1000°C with one heating cycle. The dominant gas species that evolved during thermal desorption were the carbon oxides, ie CO

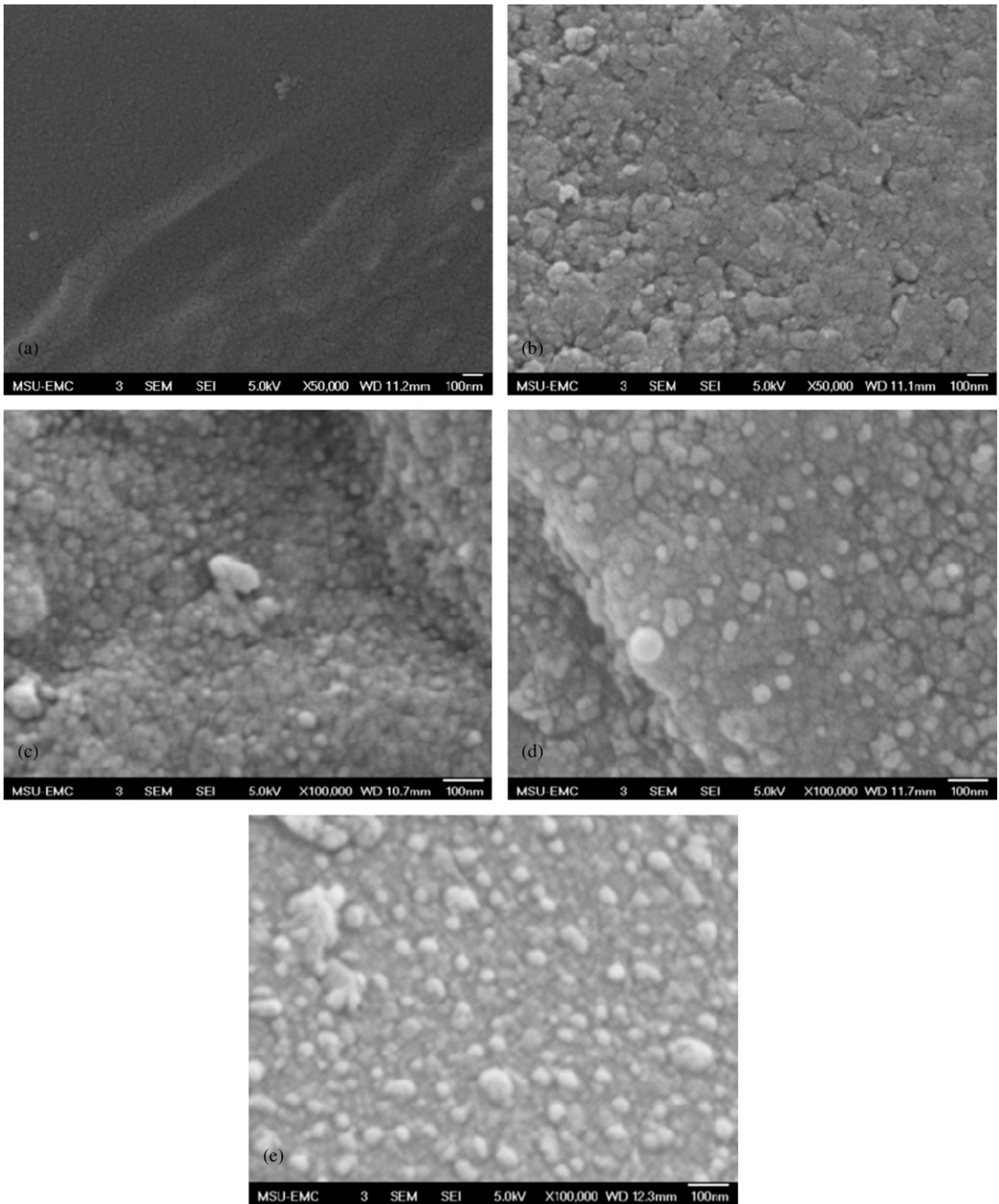


Figure 3. Scanning electron microscope images of pine wood and its bio-char thermally treated at different temperatures: (a) raw pine wood, (b) char heated at 500°C, (c) 700°C, (d) 900°C, and (e) 1000°C.

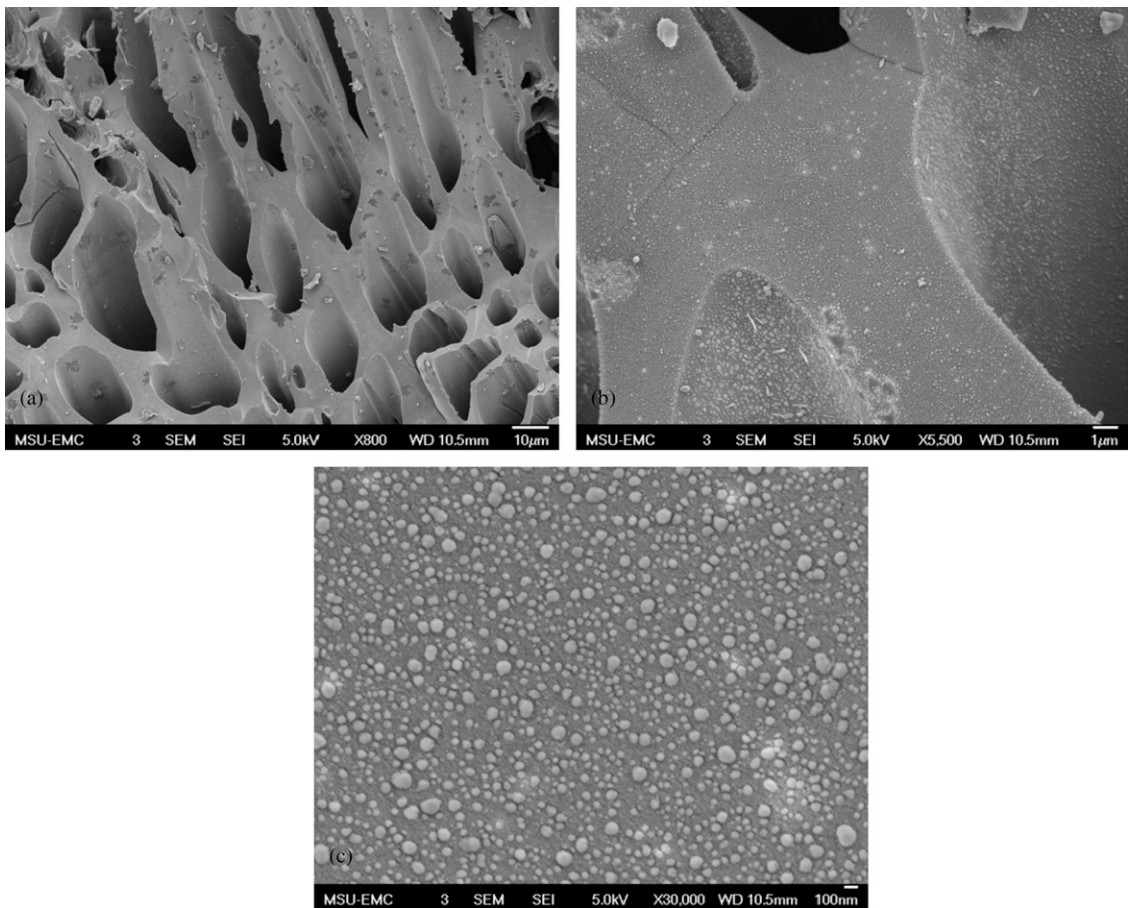


Figure 4. Scanning electron microscope images of bio-chars thermally treated at 1000°C with different magnifications of (a) 800 \times , (b) 5500 \times , and (c) 30,000 \times .

and CO₂. Oxygen-containing functional groups decomposed mostly as CO, CO₂, and H₂O. Surface complexes yielding CO₂ groups decomposed at three different temperatures corresponding to three types of functional groups (carboxylic acids, carboxylic anhydrides, and lactones). Figure 8 shows a broad CO₂ peak between 100 and 680°C with the concentration level up to 5 vol% (Yan et al 2013) in the purging gas. This peak can be deconvoluted to three peaks; the low-temperature peak (100–400°C) is assigned to the decomposition of carboxylic acids ($\text{—COOH} \rightarrow \text{CO}_2$), and the high-temperature CO₂ evolution peaks are attributed to carboxylic anhydrides (300–630°C) and lactones (390–680°C) (Figueiredo et al 1999).

The CO-yielding groups are also represented by two distinct groups of peaks corresponding to carboxylic anhydrides (300–630°C) and ether structures ($\approx 700^\circ\text{C}$) (Figueiredo et al 1999). The peak concentrations of CO in the carrier gas were 6% ($\approx 600^\circ\text{C}$) and 9% ($\approx 700^\circ\text{C}$) (Fig 8). A relatively higher level of CO than CO₂ was observed during the thermal decomposition of pinewood char because most of the functional groups related to CO₂ were decomposed during the pine wood fast pyrolysis process. The peak of H₂O released at low temperatures was generally attributed to the removal of physisorbed H₂O (room temperature to 200°C). The peak at high temperatures ($\approx 530^\circ\text{C}$) was assigned to evolution of

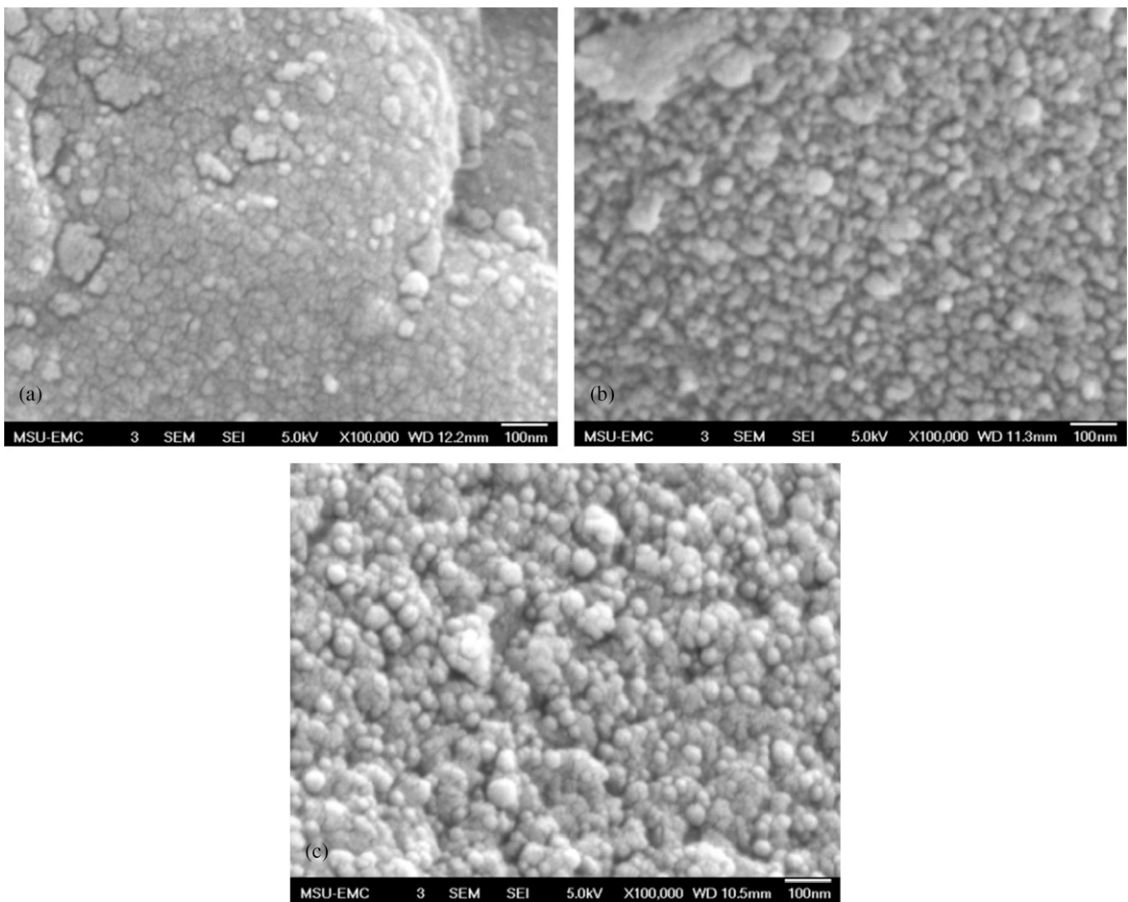


Figure 5. Scanning electron microscope images of bio-chars thermally treated at 1000°C (a) without extended time and with extended (b) 3 and (c) 5 h.

H₂O hydrogen-bonded to oxygen complexes, to condensation of phenolic groups, or to dehydration reactions of neighboring carboxylic groups to give carboxyl anhydrides. Figure 8 demonstrates that most of the oxygen-containing functional groups in the char were eliminated after heating at 1000°C. The CH₄ peak at 615°C originated from decomposition of the methyl group attached to aromatic units. Significant amounts of hydrogen in wood are chemically bonded to the backbone of cellulose, hemicellulose, and lignin through C-H bonds. The C-H bond is very stable but breaks with high-temperature heating. Nevertheless, complete desorption of hydrogen does not happen at temperatures below 1000°C. Usually, the biomass fast pyrolysis process is per-

formed at about 500°C. Therefore, significant amounts of hydrogen in biomass are left in residue char. Part of the hydrogen on a char exists as chemisorbed H₂O or as surface functionalities (eg carboxylic acids, phenolic groups, amines), and more is bonded directly to carbon atoms as part of aromatic or aliphatic structures. Heat treatment in an inert atmosphere eliminates part of the hydrogen via surface reduction. Figure 8 shows hydrogen desorption began at 400°C, increased gradually, and reached a maximum level of 20 vol% at 775°C. Then it decreased to 6.75 vol% at 1000°C (Yan et al 2013).

Figure 9 shows the evolution of H₂, CH₄, H₂O, CO, and CO₂ detected while the chars underwent

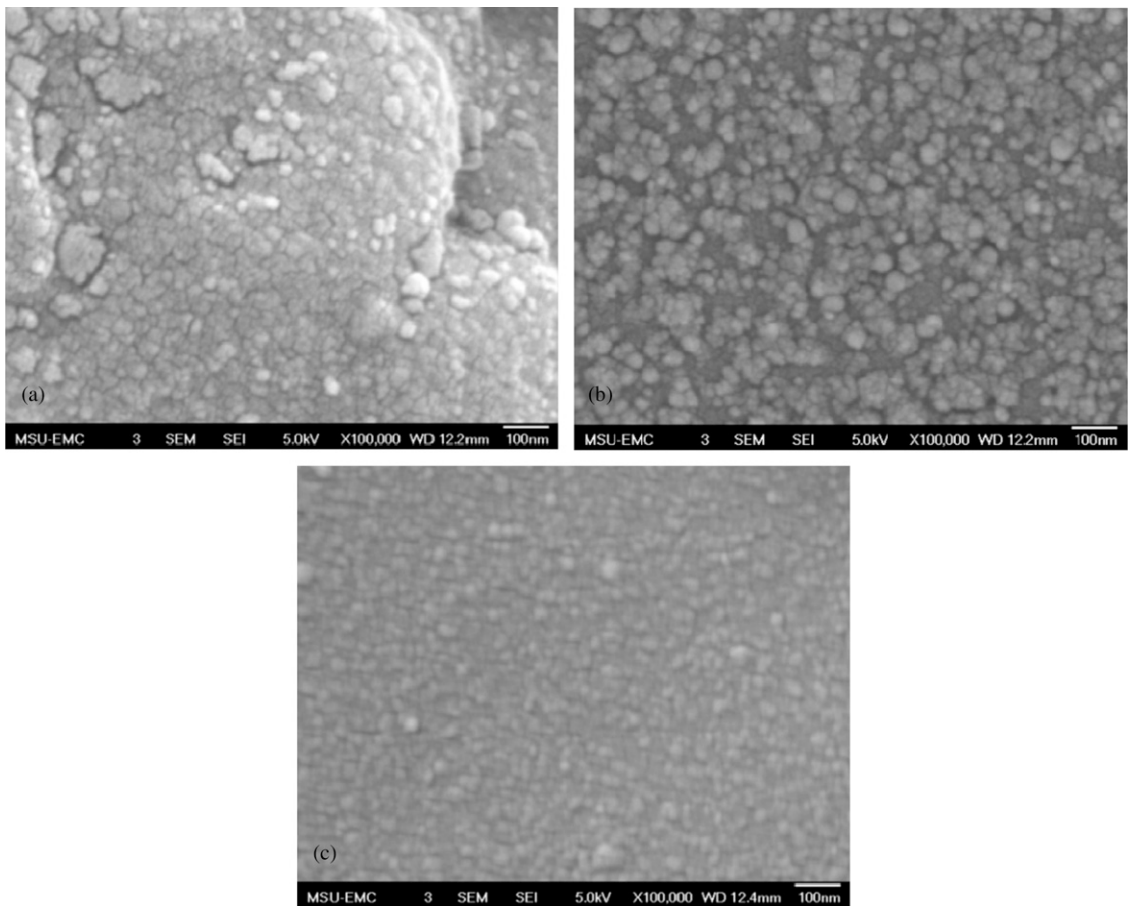


Figure 6. Scanning electron microscope images of bio-chars thermally treated at 1000°C with (a) one cycle, (b) three cycles, and (c) five cycles.

five cycles of temperature-programmed thermal treatment. Traces of H_2 and CO were detected in the second and higher cycles. Intensities of both H_2 and CO were much lower than that formed in the first cycle, and intensities decreased with increasing numbers of thermal treatment cycles. No CH_4 , H_2O , or CO_2 was detected after the second thermal cycle. Oxygen-containing groups were the most common functionalities present on the carbon surface. Carboxylic acid liberated CO_2 when it underwent decomposition, whereas carboxylic anhydrides produced both CO and CO_2 peaks. Phenols, ethers, and quinones produced a CO peak. After the first cycle, carboxylic acid, carboxylic anhydrides, and phenols should be

completely destroyed. Ether and quinone structures are more stable; they undergo gradual decomposition and can persist for many cycles of thermal treatment.

Usually, hydrogen is present on a char matrix as chemisorbed H_2O as surface functionalities (eg carboxylic acids, phenolic groups, amines) or is bonded directly to carbon atoms as part of aromatic or aliphatic structures. Heat treatment in an inert atmosphere eliminates part of the hydrogen via surface reduction. Hydrogen in chemisorbed H_2O and surface functionalities is easily decomposed and desorbed when the char is heated, whereas the C-H bond in aromatic or

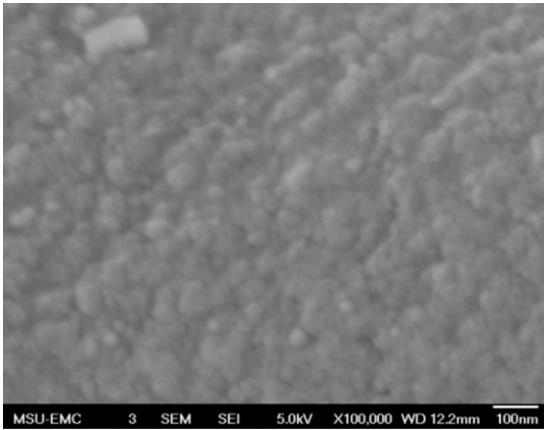


Figure 7. Scanning electron microscope image of biochars thermally treated at 1000°C with a flow of hydrogen and nitrogen mixture.

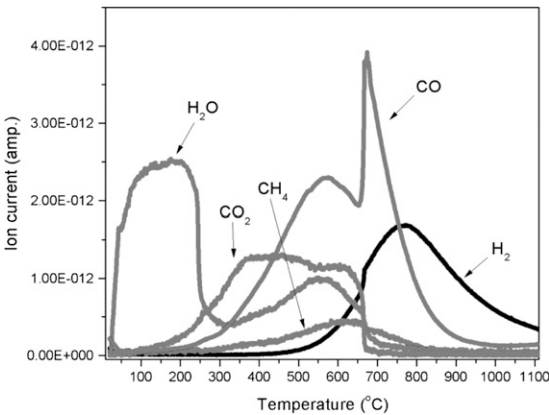


Figure 8. H_2 , CH_4 , H_2O , CO , and CO_2 evolution for the temperature-programmed thermal treatment of pine chars heated to 1000°C for one cycle at a heating rate of 10°C/min and with a nitrogen flow rate of 50 mL/min.

aliphatic structures is very stable but breaks when heating to approximately 1000°C. Nevertheless, complete desorption of hydrogen does not happen at temperatures below 1100°C during TPD.

Effect of purge gas. Figure 10 indicates that there was one hydrogen consumption peak at approximately 600°C and one hydrogen evolution peak at about 800°C. These peaks were attributed to the sequential, dissociative adsorp-

tion of hydrogen that occurs first to form C-H, then C-(H_2), then C-(H_3), followed by formation of CH_4 . The hydrogen desorption peak centered at $\approx 800^\circ\text{C}$ is assigned to the breaking down of the C-H bond in the bio-char matrix during thermal treatment. Hydrogen is released when the C-H bond is broken.

Thermogravimetric Analysis

Figure 11 shows thermogravimetric and differential thermal thermogravimetric curves of the pine char heated at a rate of 10°C/min in an N_2 atmosphere. A continuous weight loss associated with increasing temperature was observed, which may be attributed to breaking of chemical linkages and removal of volatile products from the char. There are six possible steps of weight loss. The initial weight loss corresponds to the loss of physically adsorbed H_2O and occurs between ambient temperature and 110°C with a peak loss at 74°C. It is followed by a plateau region for the rate of weight loss from 110-190°C.

The first significant weight loss, at about 190-350°C, corresponds to the decomposition of all the carboxylic acids and part of the carboxylic anhydrides and lactones. These results indicate that oxygen functional groups start to decompose in this temperature zone, which leads to the aromatization of the char matrix. The greatest weight loss of the char occurred in the temperature zone of 350-700°C. This mass loss step mainly corresponds to the decomposition of the rest of the carboxylic anhydrides and lactones, part of the phenols, quinone, and ether structures released as volatile products, CO_2 , CO , CH_4 , H_2O , and H_2 .

The third significant mass loss happened at 700-900°C. In this zone, the mass loss was mainly attributed to the decomposition of phenols, quinone, ether, and C-H groups, which produce CO and H_2 as the main products (Fig 8). Above 900°C, the mass decreased gradually as the temperature increased up to 1000°C and only trace

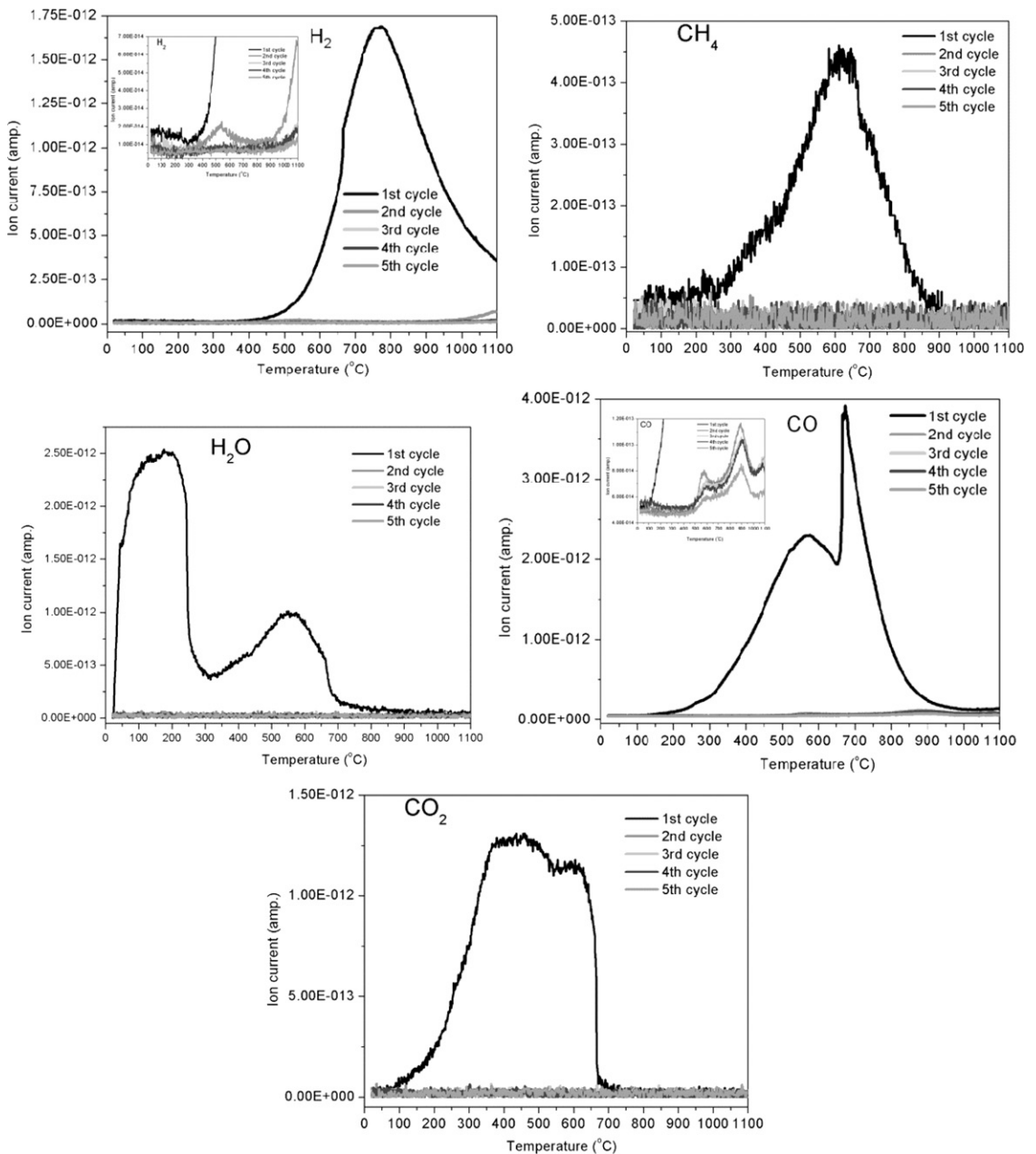


Figure 9. H₂, CH₄, H₂O, CO, and CO₂ evolution in five cycles for the temperature-programmed thermal treatment of pine chars heated to 1000°C for five cycles at a heating rate of 10°C/min and with a nitrogen flow rate of 50 mL/min.

amounts of H₂ were released. The carbonization process of the char was completed because almost all the oxygen-containing functional groups were eliminated from the char.

Elemental Composition of Nanospheres

To analyze the elemental composition of the nanospheres, SEM-EDX (Fig 12) was used to identify the surface elemental composition of

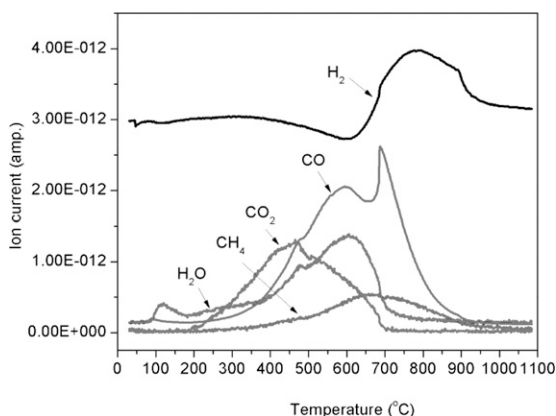


Figure 10. H_2 , CH_4 , H_2O , CO , and CO_2 evolution for the temperature-programmed thermal treatment of bio-chars with 10 vol% H_2 -Ar (50 mL/min) as the purging gases and $10^\circ C/min$ to $1000^\circ C$.

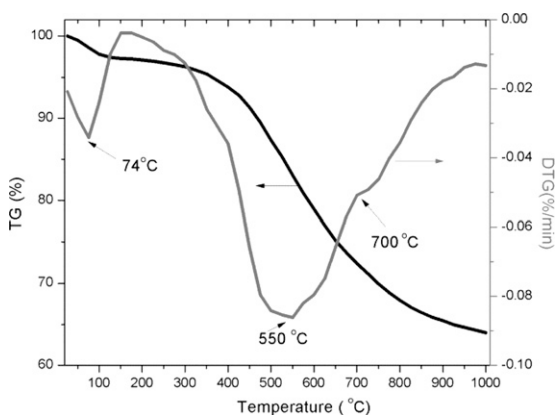


Figure 11. Thermogravimetric (TG) and differential thermal thermogravimetric (DTG) curves of pine char heated at a rate of $10^\circ C/min$ in N_2 atmosphere.

the pretreated char. The results are shown in Table 1 and demonstrate that the nanospheres were mainly composed of carbon (>95%). Thus, carbon nanospheres were formed during thermal treatment of the bio-char.

Nanocarbon Particle Characterization

Figure 13 shows TEM images of nanoparticles washed off from pine chars thermally treated at $1000^\circ C$ for 3 h. Nanocarbon spheres are the

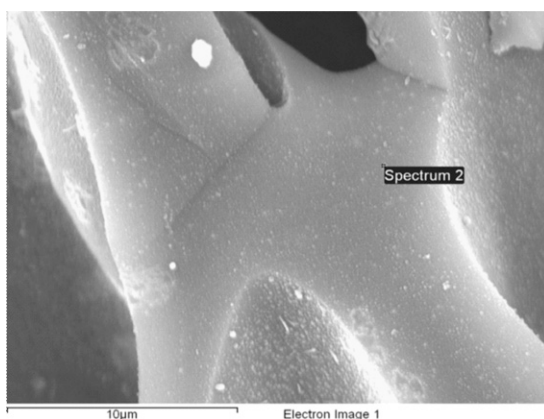


Figure 12. Scanning electron microscope energy-dispersive X-ray spectra of a bio-char sample thermally treated at $1000^\circ C$.

main content of the sample, and these particles had diameters between 20 and 100 nm. Large amounts of nanocarbon spheres mixed with amorphous carbon or graphene film (Fig 13a-b) were found for the pine chars.

CONCLUSIONS

The influence of thermal treatment conditions of temperature, reaction cycle and time, and purge gas type on nanocarbon formation over the bio-char from fast pyrolysis and the effect of thermal reaction cycle and purge gas type on the bio-char surface functional groups were investigated by TPD and TPR methods. SEM image analyses of the morphology of bio-chars heat-treated at different temperatures indicated that some nanosphere formation started on the surface of the bio-char under an activation temperature of $700^\circ C$. A greater number of nanospheres occurred when the temperature was increased to $900^\circ C$. With further increase of

Table 1. Scanning electron microscope energy-dispersive X-ray spectroscopy results of produced chars.

Element	Weight (%)	Atomic (%)
Carbon	95.41	96.65
Oxygen	4.21	3.21
Sodium	0.12	0.07
Potassium	0.26	0.08
Total	100.00	

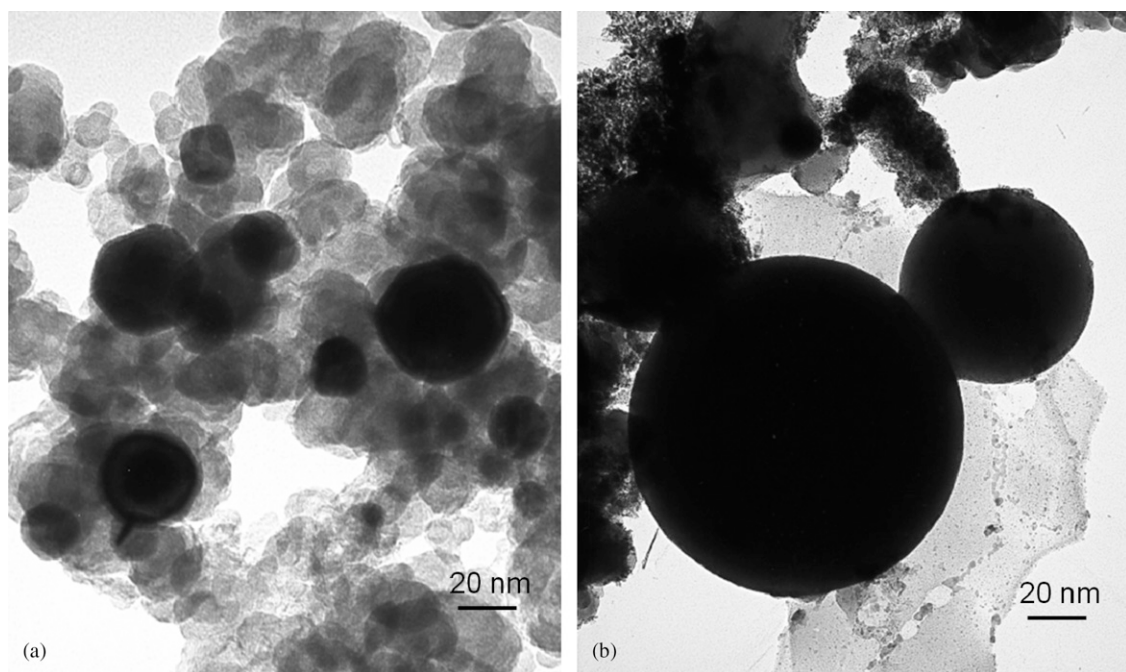


Figure 13. Transmission electron microscopy image of carbon particles washed off from pine woody chars produced at final temperature of 1000°C for 3 h with a heating rate of 10°C/min and a nitrogen flow rate of 500 mL/min.

activation temperature to 1100°C, the bio-char surface filled with a layer of nanospheres between 20 and 100 nm in diameter. SEM-EDX results confirmed that these observed nanospheres were carbon-based nanoparticles formed during thermal treatment of the bio-char.

SEM image analyses of the morphology of biochars heat-treated at different thermal treatment cycles and times indicated that more carbon nanospheres formed with an increased number of thermal cycles and thermal treatment hours. TPR run results indicated that there were few or no nanoparticles observed over the surface of the char produced when the purge gas contained hydrogen. The surface of the hydrogen-treated char was porous.

TPD results indicated that five species of H₂, H₂O, CH₄, CO, and CO₂ in their gas phases evolved from pine char heated to 1000°C at the first heating cycle. H₂ and CH₄ peaked at 750 and 615°C, respectively. Both H₂O and CO had two peaks, and CO₂ had a broad peak. Only

trace amounts of H₂ and CO were detected in the second cycle. No CH₄, H₂O, or CO₂ was detected after the second thermal cycle.

ACKNOWLEDGMENT

Approved for publication as Journal Article No. FP 729 of the Forest and Wildlife Research Center, Mississippi State University.

REFERENCES

- Azargohar R, Dalai AK (2006) Biochar as a precursor of activated carbon. *Appl Biochem Biotechnol* 131(1-3): 762-773.
- Balaban A, Klein D, Liu X (1994) Graphitic cones. *Carbon* 32(2):357-359.
- Dalai AK, Azargohar R (2007) Production of activated carbon from biochar using chemical and physical activation: Mechanism and modeling. *ACS Sym Ser* 954, Materials, Chemicals, and Energy from Forest Biomass, American Chemical Society, Washington, DC. pp. 463-476.
- Dasgupta K, Joshi JB, Banerjee S (2011) Fluidized bed synthesis of carbon nanotubes—A review. *Chem Eng J* 171(3):841-869.

- Demirbas A, Arslan G, Pehlivan E (2006) Recent studies on activated carbons and fly ashes from Turkish resources. *Energy Source, Part A: Recovery, Utilization, and Environmental Effects* 28(7):627-638.
- Figueiredo JL, Pereira MFR, Freitas MMA, Orfao JJM (1999) Modification of the surface chemistry of activated carbons. *Carbon* 37(9):1379-1389.
- Geim AK, Novoselov KS (2007) The rise of graphene. *Nat Mater* 6(3):183-191.
- Hüttinger KJ, Michenfelder AW (1987) Molecular structure of a brown coal. *Fuel* 66:1164-1170.
- Hwang KC (2010) Recent progress in the preparation and application of carbon nanocapsules. *J Phys D Appl Phys* 43(37):1-13.
- Ingram L, Mohan D, Bricka M, Steele P, Strobel D, Crocker D, Mitchell B, Mohammad J, Cantrell K, Pittman CU Jr. (2008) Pyrolysis of wood and bark in an auger reactor: Physical properties and chemical analysis of the produced bio-oils. *Energy Fuels* 22:614-625.
- Li Q, Yan H, Zhang J, Liu Z (2004) Effect of hydrocarbons precursors on the formation of carbon nanotubes in chemical vapor deposition. *Carbon* 42:829-835.
- Llobet E (2013) Gas sensors using carbon nanomaterials: A review. *Sens Actuators B Chem* 179:32-45.
- Lubineau G, Rahaman A (2012) A review of strategies for improving the degradation properties of laminated continuous-fiber/epoxy composites with carbon-based nanoreinforcements. *Carbon* 50(7):2377-2395.
- Mezohegyi G, van der Zee FP, Font J, Fortuny A, Fabregat A (2012) Towards advanced aqueous dye removal processes: A short review on the versatile role of activated carbon. *J Environ Manage* 102(15):148-164.
- Miao JY, Hwang DW, Narasimhulu KV, Lin PI, Chen YT, Lin SH, Hwang LP (2004) Synthesis and properties of carbon nanospheres grown by CVD using Kaolin supported transition metal catalysts. *Carbon* 42:813-822.
- Mohan D, Pittman CU, Steele PH (2006) Pyrolysis of wood/biomass for bio-oil: A critical review. *Energy Fuels* 20(3):848-889.
- Morgan P (2005) Carbon fibers and their composites. ISBN-13: 9780824709839. CRC Press, Boca Raton, FL. 1200 pp.
- Özçimen D, Ersoy-Meriçboyu A (2008) A study on the carbonization of grape seed and chestnut shell. *Fuel Process Technol* 89(11):1041-1046.
- Pierson HO (2006) Handbook of carbon, graphite, diamond and fullerenes—Properties, processing and applications. William Andrew Publishing/Noyes Publications, Park Ridge, NJ.
- Qureshi A, Kang WP, Davidson JL, Gurbuz Y (2009) Review on carbon-derived, solid-state, micro and nano sensors for electrochemical sensing applications. *Diamond Related Materials* 18(12):1401-1420.
- Satya Sai PM, Ahmed J (1997) Production of activated carbon from coconut shell char in a fluidized bed reactor. *Ind Eng Chem Res* 36(9):3625-3630.
- Serp P, Figueiredo JL (2008) Carbon materials for catalysis. John Wiley & Sons, Hoboken, NJ. 579 pp.
- Shahin MM (1965) Reaction of elementary carbon and hydrogen in high-frequency discharge. *Nature* 195:992-993.
- Wang Q, Li H, Chen LQ, Huang XJ (2001) Monodispersed hard carbon spherules with uniform nanopores. *Carbon* 39:2211-2215.
- Yan Q, Wan C, Liu J, Gao J, Yu F, Zhang J, Cai Z (2013) Iron nanoparticles *in situ* encapsulated in biochar-based carbon as an effective catalyst for the conversion of biomass-derived syngas to liquid hydrocarbons. *Green Chem* 15:1631-1640.